

# Implications of Wind-Assisted Aerial Navigation for Titan Mission Planning and Science Exploration

A. Elfes (1), K. Reh (1), P. Beauchamp (1), N. Fathpour (1), L. Blackmore (1), C. Newman (2), Y. Kuwata (1), M. Wolf (1), C. Assad (1)

(1) Jet Propulsion Laboratory, California Institute of Technology, Pasadena, CA, USA

(elfes@jpl.nasa.gov, phone: +1-818-393-6487)

(2) Geological and Planetary Sciences, California Institute of Technology, Pasadena, CA, USA

*Abstract*—The recent Titan Saturn System Mission (TSSM) proposal incorporates a montgolfière (hot air balloon) as part of its architecture. Standard montgolfière balloons generate lift through heating of the atmospheric gases inside the envelope, and use a vent valve for altitude control. A Titan aerobot (robotic aerial vehicle) would have to use radioisotope thermoelectric generators (RTGs) for electric power, and the excess heat generated can be used to provide thermal lift for a montgolfière. A hybrid montgolfière design could have propellers mounted on the gondola to generate horizontal thrust; in spite of the unfavorable aerodynamic drag caused by the shape of the balloon, a limited amount of lateral controllability could be achieved. In planning an aerial mission at Titan, it is extremely important to assess how the moon-wide wind field can be used to extend the navigation capabilities of an aerobot and thereby enhance the scientific return of the mission. In this paper we explore what guidance, navigation and control capabilities can be achieved by a vehicle that uses the Titan wind field. The control planning approach is based on passive wind field riding. The aerobot would use vertical control to select wind layers that would lead it towards a predefined science target, adding horizontal propulsion if available. The work presented in this paper is based on aerodynamic models that characterize balloon performance at Titan, and on TitanWRF (Weather Research and Forecasting), a model that incorporates heat convection, circulation, radiation, Titan haze properties, Saturn’s tidal forcing, and other planetary phenomena. Our results show that a simple unpropelled montgolfière without horizontal actuation will be able to reach a broad array of science targets within the constraints of the wind field. The study also indicates that even a small amount of horizontal thrust allows the balloon to reach any area of interest on Titan, and to do so in a fraction of the time needed by the unpropelled balloon. The results show that using the Titan wind field allows an aerobot to significantly extend its scientific reach, and that a montgolfière (unpropelled or propelled) is a highly desirable architecture that can very significantly enhance the scientific return of a future Titan mission.

## TABLE OF CONTENTS

1. INTRODUCTION .....	1
2. TITAN WIND MODEL.....	2
3. NAVIGATION PLANNING APPROACH .....	2
4. WIND-ASSISTED NAVIGATION ON TITAN .....	3
5. EVALUATION OF RESULTS.....	6
6. CONCLUSIONS .....	7
7. ACKNOWLEDGMENTS .....	7
REFERENCES .....	7

## 1. INTRODUCTION

The recent Titan Saturn System Mission (TSSM) proposal [1] incorporates a montgolfière (hot air balloon) as part of its architecture. Standard montgolfière balloons generate lift through heating of the atmospheric gases inside the envelope, and use a vent valve for altitude control (Fig. 1). A Titan aerobot (robotic aerial vehicle) would have to use radioisotope thermoelectric generators (RTGs) for electric power, and the excess heat generated can be used to provide thermal lift for a montgolfière. This concept was baselined in the recent NASA/ESA Titan Saturn System Mission (TSSM) proposal [1]. A hybrid montgolfière design could have propellers mounted on the gondola to generate horizontal thrust; in spite of the unfavorable aerodynamic drag caused by the shape of the balloon, a limited amount of lateral controllability can be achieved.

In planning an aerial mission at Titan, it is extremely important to assess how the moon-wide wind field can be used to extend the navigation capabilities of an aerobot, so that widely dispersed science targets can be visited (Fig. 2), thereby enhancing the scientific return of the mission. In this paper we explore what guidance, navigation and control capabilities can be achieved by a vehicle that uses the Titan wind field. The control planning approach is based on passive wind field riding. The aerobot would use vertical control to select wind layers that would lead it towards a predefined science target, adding horizontal propulsion if available. The work presented in this paper is based on

aerodynamic models that characterize balloon performance at Titan, and on a Titan WRF (Weather Research and Forecasting) model [2] that incorporates heat convection, circulation, radiation, Titan haze properties, Saturn’s tidal forcing, and other planetary phenomena.



**Figure 1 – A Titan Montgolfiere balloon. Artist’s concept (Tibor Balint).**

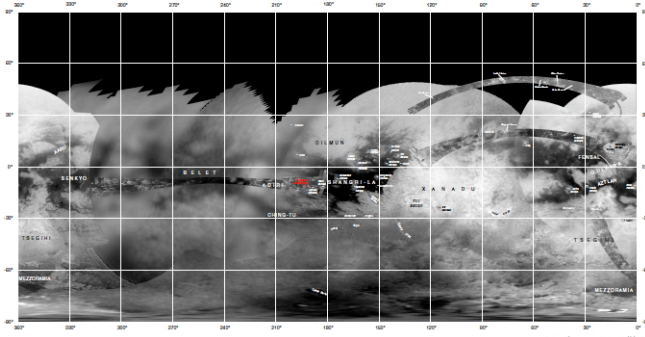


**Figure 2 – Map of interesting sites on Titan. Map Credit: NASA/JPL/Space Science Institute.**

## 2. TITAN WIND MODEL

The Titan wind model we use in our analysis is described in [2]. TitanWRF is a global model of Titan’s atmosphere, extending from the surface to approximately 400 km. Based on a global version of the terrestrial WRF (Weather Research and Forecasting) model, TitanWRF basically solves the primitive equations of atmospheric physics (“ $F = ma$ ” in a rotating frame, while ensuring conservation of mass and energy) discretized onto a three-dimensional grid. TitanWRF has been fully adapted to Titan conditions (low gravity, slow rotation rate, atmospheric composition, etc.) and is typically run with 5 degrees between horizontal grid points and with 55 vertical levels (spaced more closely within Titan’s troposphere, below approx. 40 km). The model includes parameterizations of turbulent mixing, sub-surface heat diffusion, surface energy and momentum exchange, and a radiative transfer scheme for Titan’s thick, hazy N<sub>2</sub>-CH<sub>4</sub> atmosphere. The radiative transfer scheme

used in TitanWRF is largely based on the work described in [3]. TitanWRF also includes the seasonal and diurnal variation in incident solar energy at each location.

Finally, TitanWRF includes the gravitational accelerations due to Titan’s eccentric orbit around Saturn. This produces a time-dependent change (“tide”) in the gravitational forcing which modifies horizontal wind directions and speeds, particularly in the lower atmosphere where background wind speeds are quite low. These accelerations repeat once per orbit, and so have a period of approx. 1 Titan solar day. In TitanWRF we assume that the solar and gravitational forcings stay in phase with each other at all times. In reality the phase between them shifts gradually through a full 360 degrees over the course of a Titan year (673 Titan days), but the thermal tide is far weaker so this should be relatively unimportant. TitanWRF does not include spatial variations in surface properties (such as topography, roughness, albedo or thermal inertia) due to the limited datasets available for each of them. Further details on how TitanWRF is used in this study are available in [4].

## 3. NAVIGATION PLANNING APPROACH

We assume that we have a general set of dynamic equations for the montgolfiere in a time-varying wind field of the form:  $dx/dt = f[x(t);u(t); t]$ , where  $u(t)$  are the heating, venting and horizontal actuation control inputs applied at time  $t$ , and  $x(t)$  is the state of the montgolfiere at time  $t$ . Equations in this form are derived by [5] using the thermal and dynamics balloon models of [6]. In this case, the state includes the temperature and volume of the balloon, as well as the three-dimensional position and velocity of the montgolfiere. The dynamics of the montgolfiere rely on a predictive model of the winds at any location  $r$  and time  $t$ . We assume we have such a model in the general form  $w[r; t]$ , as described in Section 2.

The path planning and reachability problem is stated as follows: given a montgolfiere with dynamics  $f[.]$ , initially at location  $r_0$ , and a wind model  $w[.]$ , determine, for every possible end location  $r_f$ , the minimum time to reach  $r_f$  and the sequence of control inputs  $u[.]$  that achieves this minimum.

Aerobot navigation planning is done by solving a discretized approximation of the problem described above. The planning problem is transformed into a graph search problem through an efficient discretization of the search space. Dijkstra’s algorithm is used to calculate the minimum-time path from the start location to every possible location in the graph. Given a graph  $G$ , the algorithm finds the minimum cost path from a start node to all other nodes in the graph [4]. Given the reach-ability results, the path planning problem can be solved by extracting the path that corresponds to the particular target node.

Our approach has been applied to the following cases:

- deterministic, static (time-invariant) wind fields
- deterministic, time-varying wind fields
- stochastic (uncertain), time-varying wind fields

As is to be expected, the computational complexity of the problem increases substantially as we go from deterministic/static to deterministic/time-varying and to stochastic/time-varying fields. At the same time, the fidelity of the results increases. A detailed discussion of the computational models used is available in [4, 7, 8].

#### 4. WIND-ASSISTED NAVIGATION ON TITAN

We now discuss the results obtained using the navigation planning algorithm outlined above. In what follows, we define a Titan (solar) day as the time taken for Titan to rotate once (roughly 16 Earth days). Titan is tidally locked, and therefore keeps roughly the same face to Saturn at all times, so one Titan day is also the time taken for it to orbit Saturn. As Titan is in orbit around Saturn, a Titan year [ $\sim 673$  Titan days] is the same as a Saturn year and lasts roughly 30 Earth years. Finally, we define a Titan hour as 1/24th of a Titan day. We describe seasons using Titan (Saturn's) angular position in its orbit around the Sun, i.e. using its planetocentric solar longitude  $L_s$ .  $L_s = 0$  is the northern spring equinox,  $L_s = 90$  the northern summer solstice, and so on. Perihelion (the time at which Saturn and thus Titan are closest to the Sun) occurs at  $L_s = 278$ , during the northern winter / southern summer.

##### *Deterministic, time-invariant wind field*

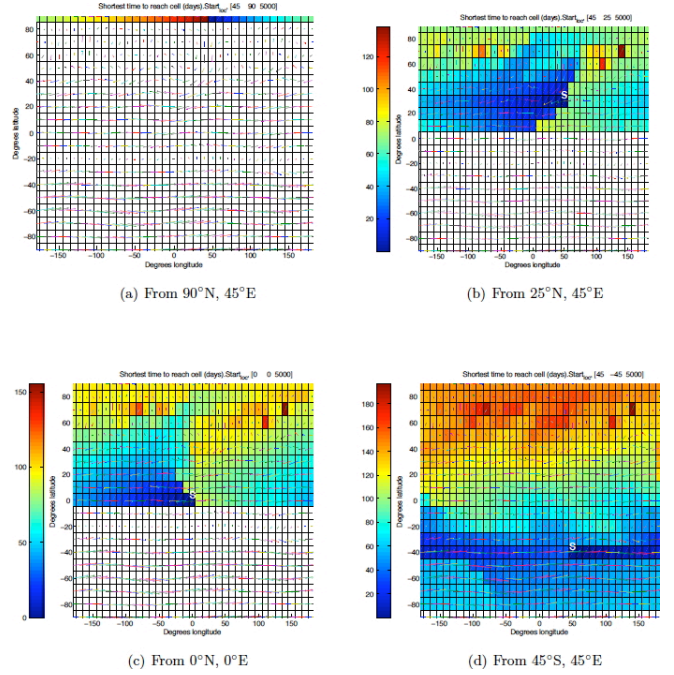
For illustrative purposes, we start with the time-invariant wind field case. Note that the results shown here are superseded by those with time-varying winds, given below.

For the following results, winds at time  $L_s = 90$  were used, corresponding to summer solstice. In the computational analysis, we used a horizontal grid of  $10^\circ$  in longitude and latitude, a vertical grid of 500 m, and a temporal discretization of 0.2 Titan days. For the results shown below, the balloon is assumed to have vertical control, and rise and sink speeds were assumed to be 0.3 m/s and 0.6 m/s, respectively. If horizontal actuation is available, we assumed a horizontal speed of 1 m/s. The whole model is parameterized, so that the analyses can be rerun with other values of these parameters.

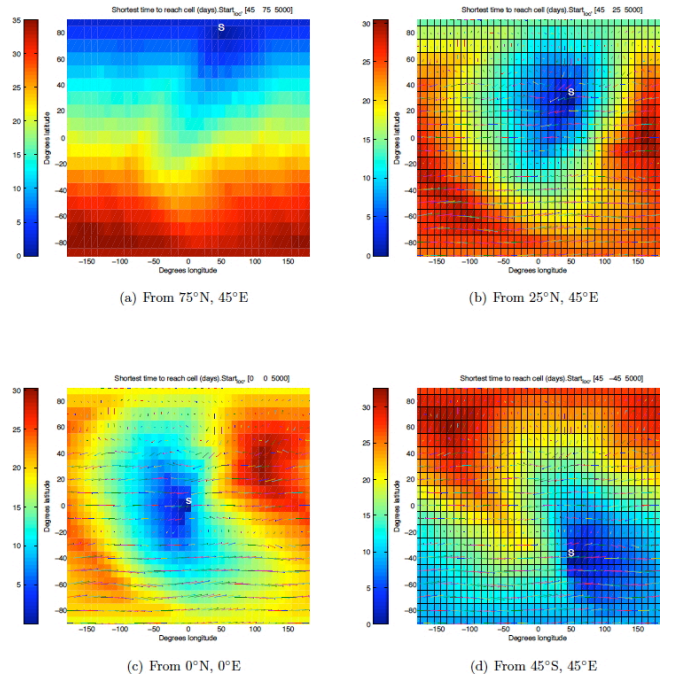
Fig. 3 shows reachability maps for Titan with no horizontal actuation at 4 different starting locations in the Titan poles, the equator and the southern hemisphere. The color coding shows how long it takes for the balloon to move from the starting location “S” to all other cells on Titan. White cells are not reachable due to unfavorable wind configurations. Transit times to a specific cell may reach values of 200 days and above.

Fig. 4 shows, in contrast, global reachability maps for static wind fields when the vehicle is assumed to have horizontal actuation. As can be seen, any place on Titan is now

reachable, and transit times to a given cell are reduced drastically.



**Figure 3 – Global reachability maps with no horizontal actuation and assuming a static wind field. The cell colors show how long it takes to reach a given cell from the indicated starting location. A white cell is not reachable.**



**Figure 4 – Global reachability maps with horizontal actuation of 1 m/s, assuming a static wind field. The cell colors show how long it takes to reach a given cell from the indicated starting location.**

*Deterministic, time-varying wind field*

Because the Titan wind field at a given location varies with time, we perform a temporal as well as a spatial discretization. Again, the computational algorithms are discussed in [4, 7, 8].

In the following results, we again have  $L_s = 90$ , corresponding to summer solstice. The same parameter values given above were used. Fig. 5 shows reachability maps for Titan with no horizontal actuation at 3 different starting locations as indicated. The color coding is the same as before. Fig. 6 shows the results obtained when the vehicle has horizontal actuation.

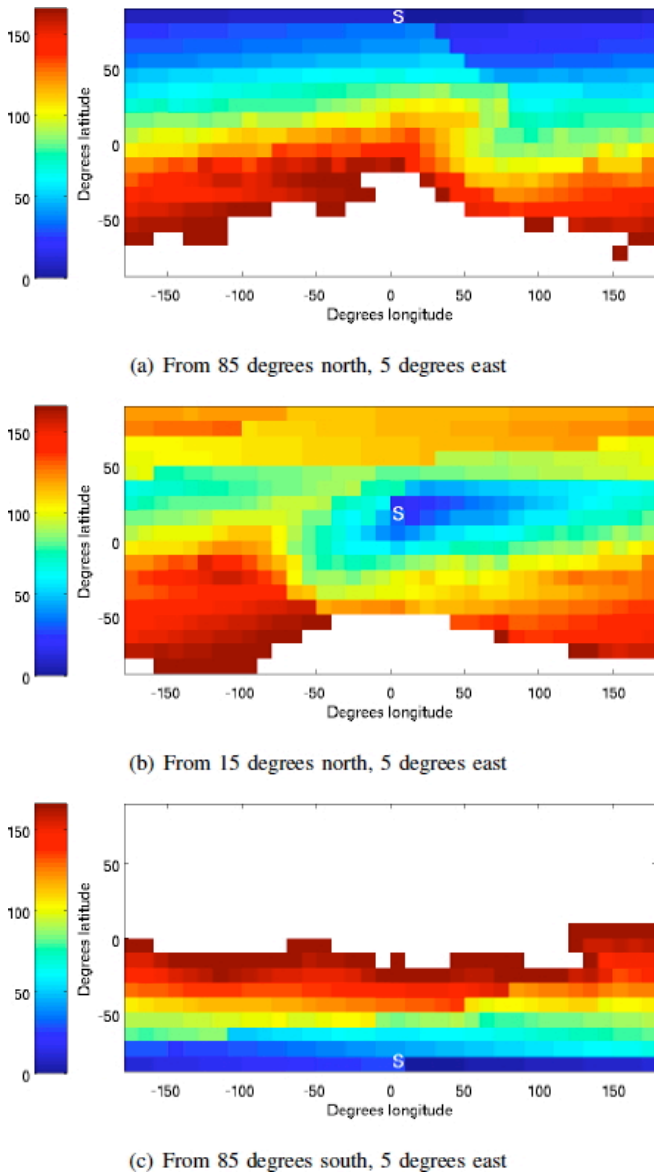


**Figure 5 – Global reachability maps without horizontal actuation, and assuming a time-varying wind field. The cell colors show the transit time required to reach a given cell from the indicated starting location. A white cell is not reachable.**

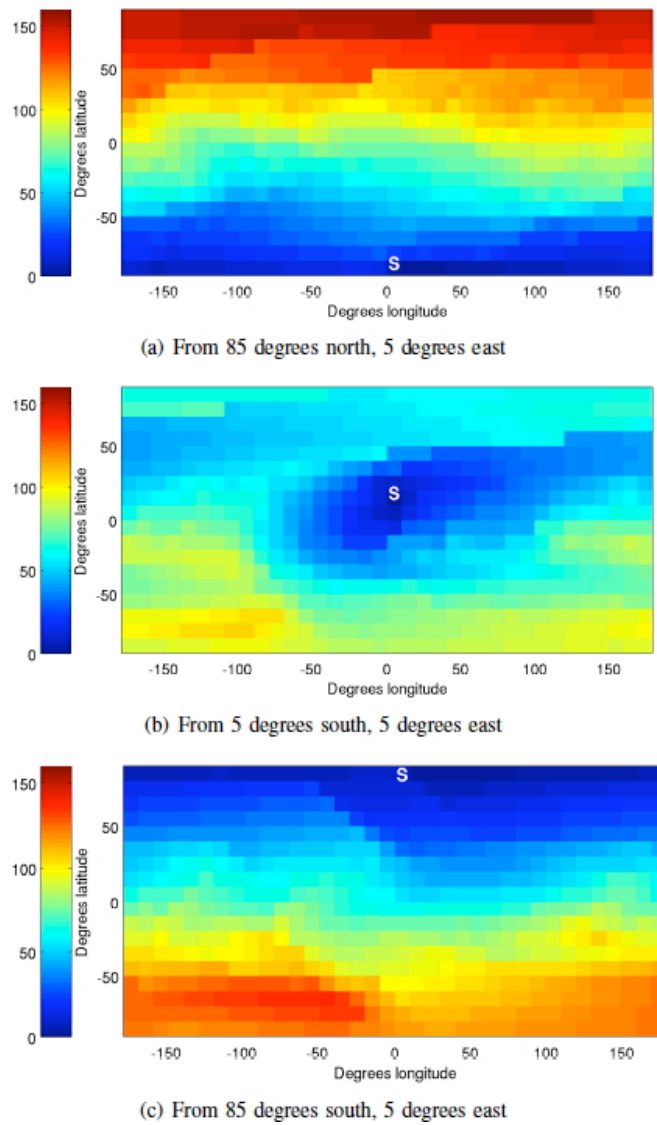


**Figure 6 – Global reachability maps without horizontal actuation, and assuming a time-varying wind field. The cell colors show the transit time required to reach a given cell from the indicated starting location. A white cell is not reachable.**

Note that depending on where the balloon starts, the reachability map varies significantly. Fig. 5 (a) and (b) show that it is difficult to reach areas around the southern pole from a starting location that is further North. This is because the wind in the north-south direction is generally weak near the southern pole.

Fig. 7 shows the percentage of the area of Titan’s surface that would be reachable in a given time. For example, 50% on the y axis means that 50% of the points on Titan’s surface could be reached in a given time if set as a destination of the shortest path problem. The plot has 24 different starting locations with the following combinations of longitude and latitude:

- 4 longitudes (175° W, 85° W, 5° E, 95° E)
- 6 latitudes (85° S, 45° S, 15° S, 15° N, 45° N, 85° N)

Because latitudinal wind field changes are much greater than longitudinal changes, the lines corresponding to the same latitude are plotted with the same color. In fact, the lines with the same color have a similar trend: if the balloon starts at 15° S (shown in red), it initially would reach only a limited area, but the reachable area grows rapidly after a few months; if the balloon starts near the southern pole (85° S), it could reach a very limited area in 5 months. This is because the north-south wind near the southern pole is weak.

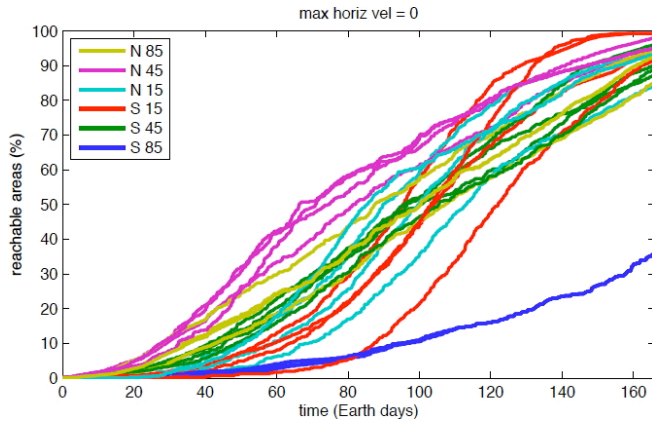


**Figure 7 – Number of cells that can be reached from 24 different starting locations. The balloon is assumed to have no horizontal actuation.**

The results for four different horizontal actuation levels are given in Fig. 8. They correspond to no actuation (0 m/s), 0.25 m/s, 0.5 m/s and 1.0 m/s.

*Stochastic, time-varying wind field*

In practice, the Titan wind field will not be known accurately before a Titan mission. In fact, even during the execution of a mission significant uncertainties corresponding the global wind field will remain. We have extended the work discussed above, adapting the algorithms for the case where the wind field is known only approximately. With uncertain wind fields, the transition from each state is no longer deterministically specified by the wind model, as it was in the approaches used above. From a given state  $s_i$ , the next state, dubbed  $s'_i$ , may be considered a random variable and a corresponding probability distribution for  $s'_i$  can be constructed over all horizontally adjacent cells. Given these transition probabilities from all states, we wish to select the actions (horizontal and vertical actuation of the Montgolfiere) that minimize time-to-goal. The approach we used is to formulate the navigation problem as a Markov Decision Process (MDP), for which a number of solution methods may be applied.

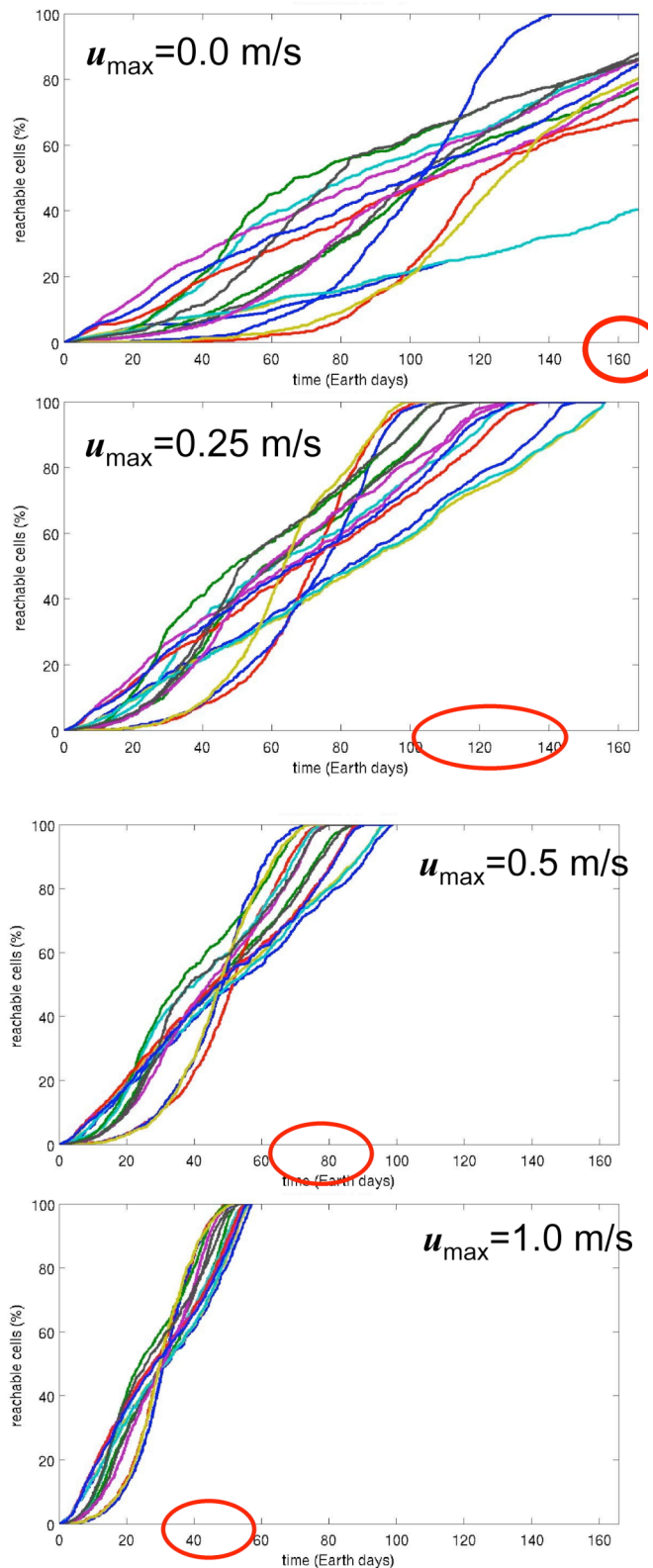


**Figure 8 – Reachability plots for 4 different horizontal actuation values: no actuation (0 m/s), 0.25 m/s, 0.5 m/s, and 1.0 m/s. The same starting points as in Fig. 7 are used.**

Let  $\tilde{w}(r_i; t)$  denote the (random) wind velocity at position  $r_i$  at time  $t$  and  $w(r_i; t)$  denote the velocity given by the TitanWRF wind field model. The direction and magnitude of  $\tilde{w}(r_i; t)$  are represented respectively by  $\theta_i$  and  $w_i$ . The wind direction  $\theta_i$  is of primary importance as it principally determines the next horizontal cell to be traversed by the vehicle. To model the uncertainty in  $\theta_i$ , we employ a von Mises distribution, an analogue of a Gaussian distribution on the circle. We set the mean of  $\theta_i$  to the angle given by the wind field model at position  $r_i$ , and the standard deviation to a constant chosen by the user. Note that the variance could also be chosen to vary by position if desired. The wind magnitude  $w_i$  uncertainty is modeled as a Gaussian, with the mean set to the value given by the wind field model, and the standard deviation set as proportional to the magnitude. Again the proportionality constant is set by the user. Further details are given in [4].

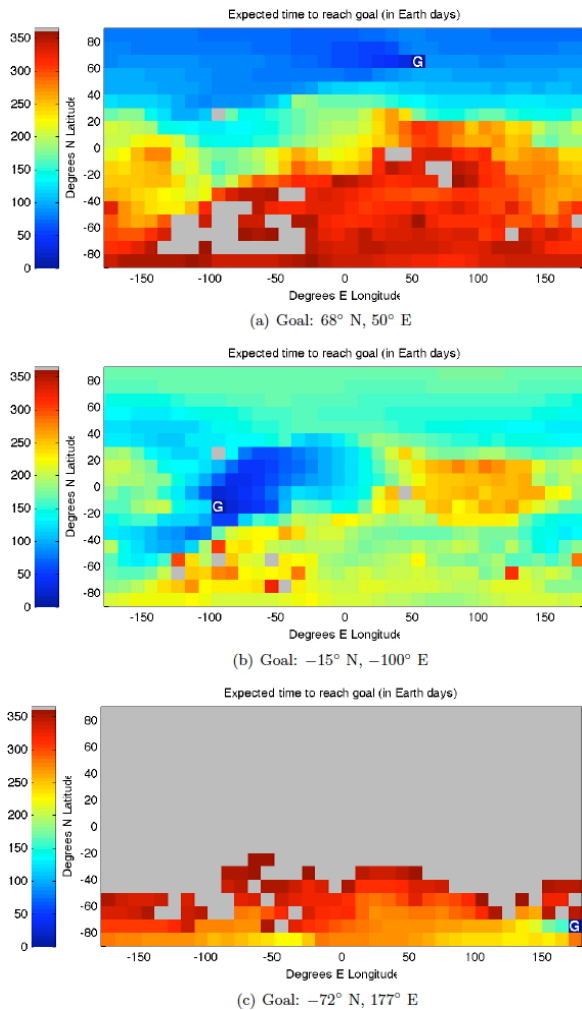


**Figure 9 - Time-to-goal plots of different goal locations for an uncertain wind field, with no horizontal actuation. Color indicates the expected time to reach the goal (labeled “G”) from each cell (in Earth days). A cross section at an altitude of 1000 m is shown. All cells with expected time-to-goal greater than 1 Earth year are colored gray.**

Fig. 9 shows the time-to-goal plots of different goal locations using the MDP solution, with no horizontal actuation. Color indicates the expected time to reach the goal (labeled “G”) from each cell (in Earth days). A cross section at an altitude of 1000 m is shown. All cells with expected time-to-goal greater than 1 Earth year are colored gray.

Fig. 10 shows the time-to-goal plots using the MDP solution, with horizontal actuation of 1 m/s. Note that the color bars are scaled very differently from those in Fig. 9.

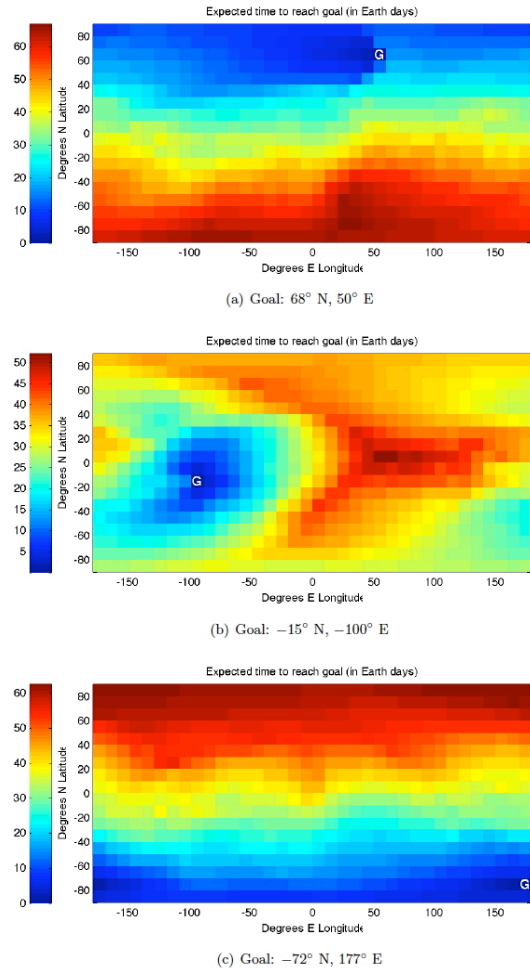


**Figure 10 - Time-to-goal plots of different goal locations for an uncertain wind field, with horizontal actuation of 1 m/s.**

## 5. EVALUATION OF RESULTS

The results presented in this paper are, of course, heavily dependent on the wind field model used, and further work is necessary to improve the robustness of the results. However, even a preliminary assessment has shown that the results obtained for different seasons, entry points and target goals are generally in agreement. Furthermore, the analysis makes abundantly clear that the uncertainty in the wind field can be

compensated for by adding a horizontal actuation capability to the vehicle.

Obviously, during an actual mission it would be necessary to improve our estimates of the Titan wind field through *in situ* wind measurements. This could be done by having the montgolfiere perform descents/ascents through the Titan atmosphere on a regular basis, estimating the wind field along the atmospheric column traversed. Wind estimation methods would be required, and these are being investigated in a separate effort [10]. The wind estimates would be used to update the Titan wind models used both by mission operations planners and by the balloon.

An overall summary of the results obtained in this study is given below for different vehicle options:

1. A Montgolfiere balloon with vertical actuation:

- Is sensitive to the atmospheric insertion location
- Is highly sensitive to the actual wind field
- Can reach science targets over ~ 50-75% of Titan
- Transit times are ~ multiple months

2. A Propelled Montgolfiere balloon with vertical and horizontal actuation:

- Is largely insensitive to entry location
- Can compensate for uncertainty in the wind field
- Can reach targets everywhere on Titan (100%)
- Transit times are ~ few weeks

## 6. CONCLUSIONS

Our results show that a simple unpropelled montgolfière without horizontal actuation will be able to reach a broad array of science targets within the constraints of the wind field. The study also indicates that even a small amount of horizontal thrust allows the balloon to reach any area of interest on Titan, and to do so in a fraction of the time needed by the unpropelled balloon. The results show that using the Titan wind field allows an aerobot to significantly extend its scientific reach, and that a montgolfière (unpropelled or propelled) is a highly desirable architecture that can very significantly enhance the scientific return of a future Titan mission.

## 7. ACKNOWLEDGMENTS

This research was carried out at the Jet Propulsion Laboratory, California Institute of Technology, under a contract with the National Aeronautics and Space Administration.

## REFERENCES

[1] Reh, K. et al. (2009) "Titan Saturn System Mission Study", NASA. Available at <http://opfm.jpl.nasa.gov/titansaturnsystemmissiontssm>.

[2] M. I. Richardson, A. D. Toigo, and C. E. Newman, "PlanetWRF: A general purpose, local to global numerical model for planetary atmospheric and climate dynamics," *Journal of Geophysical Research*, vol. 112, 2007.

[3] C. McKay, J. Pollack, and R. Courtin, "The thermal structure of Titan's atmosphere," *Icarus*, vol. 80, 1989.

[4] L. Blackmore, N. Fathpour, C. Newman, A. Elfes, K. Reh, Y. Kuwata, M. Wolf, C. Assad. "Path Planning and Global Reachability for Planetary Exploration Balloons". JPL Technical Report D-61013, Pasadena, May 2009.

[5] T. Das, R. Mukerjee, and J. Cameron, "Optimal trajectory planning for hot-air balloons in linear wind fields", *AIAA Journal of Guidance, Control and Dynamics*, vol. 3, no. 26, 2003.

[6] L. A. Carlson and W. J. Horn, "New thermal and trajectory model for high-altitude balloons", *Journal of Aircraft*, vol. 20, no. 6, 1983.

[7] Blackmore, L. et al. (2009) "Path Planning and Global Reachability for Planetary Exploration with Montgolfiere Balloons", submitted to ICRA 2010.

[8] Y. Kuwata, L. Blackmore, M. Wolf, N. Fathpour, C. Newman, and A. Elfes. "Decomposition Algorithm for Global Reachability Analysis on a Time-Varying Graph with an Application to Planetary Exploration", *Proceedings of the 2009 IEEE/RSJ International Conference on Intelligent Robots and Systems (IROS 2009)*, St. Louis, Missouri, October 2009.

[9] A. Elfes, K. Reh, P. Beauchamp, N. Fathpour, L. Blackmore, C. Newman, Y. Kuwata, M. Wolf, and C. Assad. "Wind-Assisted Aerobot Navigation at Titan: Consequences for Titan Scientific Exploration and Mission Planning", *Proceedings of the European Planetary Science Congress (EPSC 2009)*, Potsdam, Germany, September 2009.

[10] A. Elfes, J. L. Hall, E. A. Kulczycki, D. S. Clouse, A. C. Morfopoulos, J. F. Montgomery, J. M. Cameron, A. Ansar, and R. J. Machuzak. "An Autonomy Architecture for Aerobot Exploration of the Saturnian Moon Titan". In *Proceedings of the 2008 IEEE Aerospace Conference, Big Sky, MT*, March 2008.